Measurement of the B_s^0 Lifetime in the Flavor-Specific Decay Channel $B_s^0 \to D_s^- \mu^+ \nu X$

V. M. Abazov,[31] B. Abbott,[67] B. S. Acharya,[25] M. Adams,[46] T. Adams,[44] J. P. Agnew,[41] G. D. Alexeev,[31] G. Alkhazov,[35] A. Alton,[56,a] A. Askew,[44] S. Atkins,[54] K. Augsten,[7] C. Avila,[5] F. Badaud,[10] L. Bagby,[45] B. Baldin,[45] D. V. Bandurin,[73] S. Banerjee,[25] E. Barberis,[55] P. Baringer,[53] J. F. Bartlett,[45] U. Bassler,[15] V. Bazterra,[46] A. Bean,[53] M. Begalli,[2] L. Bellantoni,[45] S. B. Beri,[23] G. Bernardi,[14] R. Bernhard,[19] I. Bertram,[39] M. Besançon,[15] R. Beuselinck,[40] P. C. Bhat,[45] S. Bhatia,[58] V. Bhatnagar,[23] G. Blazey,[47] S. Blessing,[44] K. Bloom,[59] A. Boehnlein,[45] D. Boline,[64] E. E. Boos,[33] G. Borissov,[39] M. Borysova,[38,l] A. Brandt,[70] O. Brandt,[20] R. Brock,[57] A. Bross,[45] D. Brown,[14] X. B. Bu,[45] M. Buehler,[45] V. Buescher,[21] V. Bunichev,[33] S. Burdin,[39,b] C. P. Buszello,[37] E. Camacho-Pérez,[28] B. C. K. Casey,[45] H. Castilla-Valdez,[28] S. Caughron,[57] S. Chakrabarti,[64] K. M. Chan,[51] A. Chandra,[72] E. Chapon,[15] G. Chen,[53] S. W. Cho,[27] S. Choi,[27] B. Choudhary,[24] S. Cihangir,[45] D. Claes,[59] J. Clutter,[53] M. Cooke,[45,k] W. E. Cooper,[45] M. Corcoran,[72] F. Couderc,[15] M.-C. Cousinou,[12] D. Cutts,[69] A. Das,[42] G. Davies,[40] S. J. de Jong,[29,30] E. De La Cruz-Burelo,[28] F. Déliot,[15] R. Demina,[63] D. Denisov,[45] S. P. Denisov,[34] S. Desai,[45] C. Deterre,[20,c] K. DeVaughan,[59] H. T. Diehl,[45] M. Diesburg,[45] P. F. Ding,[41] A. Dominguez,[59] A. Dubey,[24] L. V. Dudko,[33] A. Duperrin,[12] S. Dutt,[23] M. Eads,[47] D. Edmunds,[57] J. Ellison,[43] V. D. Elvira,[45] Y. Enari,[14] H. Evans,[49] V. N. Evdokimov,[34] A. Fauré,[15] L. Feng,[47] T. Ferbel,[63] F. Fiedler,[21] F. Filthaut,[29,30] W. Fisher,[57] H. E. Fisk,[45] M. Fortner,[47] H. Fox,[39] S. Fuess,[45] P. H. Garbincius,[45] A. Garcia-Bellido,[63] J. A. García-González,[28] V. Gavrilov,[32] W. Geng,[12,57] C. E. Gerber,[46] Y. Gershtein,[60] G. Ginther,[45,63] O. Gogota,[38] G. Golovanov,[31] P. D. Grannis,[64] S. Greder,[16] H. Greenlee,[45] G. Grenier,[17] Ph. Gris,[10] J.-F. Grivaz,[13] A. Grohsjean,[15,c] S. Grünendahl,[45] M. W. Grünewald,[26] T. Guillemin,[13] G. Gutierrez,[45] P. Gutierrez,[67] J. Haley,[68] L. Han,[4] K. Harder,[41] A. Harel,[63] J. M. Hauptman,[52] J. Hays,[40] T. Head,[41] T. Hebbeker,[18] D. Hedin,[47] H. Hegab,[68] A. P. Heinson,[43] U. Heintz,[69] C. Hensel,[1] I. Heredia-De La Cruz,[28,d] K. Herner,[45] G. Hesketh,[41,f] M. D. Hildreth,[51] R. Hirosky,[73] T. Hoang,[44] J. D. Hobbs,[64] B. Hoeneisen,[9] J. Hogan,[72] M. Hohlfeld,[21] J. L. Holzbauer,[58] I. Howley,[70] Z. Hubacek,[7,15] V. Hynek,[7] I. Iashvili,[62] Y. Ilchenko,[71] R. Illingworth,[45] A. S. Ito,[45] S. Jabeen,[45,m] M. Jaffré,[13] A. Jayasinghe,[67] M. S. Jeong,[27] R. Jesik,[40] P. Jiang,[4] K. Johns,[42] E. Johnson,[57] M. Johnson,[45] A. Jonckheere,[45] P. Jonsson,[40] J. Joshi,[43] A. W. Jung,[45] A. Juste,[36] E. Kajfasz,[12] D. Karmanov,[33] I. Katsanos,[59] M. Kaur,[23] R. Kehoe,[71] S. Kermiche,[12] N. Khalatyan,[45] A. Khanov,[68] A. Kharchilava,[62] Y. N. Kharzheev,[31] I. Kiselevich,[32] J. M. Kohli,[23] A. V. Kozelov,[34] J. Kraus,[58] A. Kumar,[62] A. Kupco,[8] T. Kurča,[17] V. A. Kuzmin,[33] S. Lammers,[49] P. Lebrun,[17] H. S. Lee,[27] S. W. Lee,[52] W. M. Lee,[45] X. Lei,[42] J. Lellouch,[14] D. Li,[14] H. Li,[73] L. Li,[43] Q. Z. Li,[45] J. K. Lim,[27] D. Lincoln,[45] J. Linnemann,[57] V. V. Lipaev,[34] R. Lipton,[45] H. Liu,[71] Y. Liu,[4] A. Lobodenko,[35] M. Lokajicek,[8] R. Lopes de Sa,[45] R. Luna-Garcia,[28,g] A. L. Lyon,[45] A. K. A. Maciel,[1] R. Madar,[19] R. Magaña-Villalba,[28] S. Malik,[59] V. L. Malyshev,[31] J. Mansour,[20] J. Martínez-Ortega,[28] R. McCarthy,[64] C. L. McGivern,[41] M. M. Meijer,[29,30] A. Melnitchouk,[45] D. Menezes,[47] P. G. Mercadante,[3] M. Merkin,[33] A. Meyer,[18] J. Meyer,[20,I] F. Miconi,[16] N. K. Mondal,[25] M. Mulhearn,[73] E. Nagy,[12] M. Narain,[69] R. Nayyar,[42] H. A. Neal,[56] J. P. Negret,[5] P. Neustroev,[35] H. T. Nguyen,[73] T. Nunnemann,[22] J. Orduna,[72] N. Osman,[12] J. Osta,[51] A. Pal,[70] N. Parashar,[50] V. Parihar,[69] S. K. Park,[27] R. Partridge,[69,e] N. Parua,[49] A. Patwa,[65,j] B. Penning,[45] M. Perfilov,[33] Y. Peters,[41] K. Petridis,[41] G. Petrillo,[63] P. Pétroff,[13] M.-A. Pleier,[65] V. M. Podstavkov,[45] A. V. Popov,[34] M. Prewitt,[72] D. Price,[41] N. Prokopenko,[34] J. Qian,[56] A. Quadt,[20] B. Quinn,[58] P. N. Ratoff,[39] I. Razumov,[34] I. Ripp-Baudot,[16] F. Rizatdinova,[68] M. Rominsky,[45] A. Ross,[39] C. Royon,[15] P. Rubinov,[45] R. Ruchti,[51] G. Sajot,[11] A. Sánchez-Hernández,[28] M. P. Sanders,[22] A. S. Santos,[1,h] G. Savage,[45] M. Savitskyi,[38] L. Sawyer,[54] T. Scanlon,[40] R. D. Schamberger,[64] Y. Scheglov,[35] H. Schellman,[48] C. Schwanenberger,[41] R. Schwienhorst,[57] J. Sekaric,[53] H. Severini,[67] E. Shabalina,[20] V. Shary,[15] S. Shaw,[41] A. A. Shchukin,[34] V. Simak,[7] P. Skubic,[67] P. Slattery,[63] D. Smirnov,[51] G. R. Snow,[59] J. Snow,[66] S. Snyder,[65] S. Söldner-Rembold,[41] L. Sonnenschein,[18] K. Soustruznik,[6] J. Stark,[11] D. A. Stoyanova,[34] M. Strauss,[67] L. Suter,[41] P. Svoisky,[67] M. Titov,[15] V. V. Tokmenin,[31] Y.-T. Tsai,[63] D. Tsybychev,[64] B. Tuchming,[15] C. Tully,[61] L. Uvarov,[35] S. Uvarov,[35] S. Uzunyan,[47] R. Van Kooten,[49] W. M. van Leeuwen,[29] N. Varelas,[46] E. W. Varnes,[42] I. A. Vasilyev,[34] A. Y. Verkheev,[31] L. S. Vertogradov,[31] M. Verzocchi,[45] M. Vesterinen,[41] D. Vilanova,[15] P. Vokac,[7] H. D. Wahl,[44] M. H. L. S. Wang,[45] J. Warchol,[51] G. Watts,[74] M. Wayne,[51] J. Weichert,[21] L. Welty-Rieger,[48] M. R. J. Williams,[49,n] G. W. Wilson,[53] M. Wobisch,[54] D. R. Wood,[55] T. R. Wyatt,[41] Y. Xie,[45] R. Yamada,[45] S. Yang,[4] T. Yasuda,[45] Y. A. Yatsunenko,[31] W. Ye,[64] Z. Ye,[45] H. Yin,[45] K. Yip,[65] S. W. Youn,[45] J. M. Yu,[56] J. Zennamo,[62] T. G. Zhao,[41] B. Zhou,[56] J. Zhu,[56] M. Zielinski,[63] D. Zieminska,[49] and L. Zivkovic[14]

(D0 Collaboration)

[1]LAFEX, Centro Brasileiro de Pesquisas Físicas, Rio de Janeiro, Brazil
[2]Universidade do Estado do Rio de Janeiro, Rio de Janeiro, Brazil
[3]Universidade Federal do ABC, Santo André, Brazil
[4]University of Science and Technology of China, Hefei, People's Republic of China
[5]Universidad de los Andes, Bogotá, Colombia
[6]Charles University, Faculty of Mathematics and Physics, Center for Particle Physics, Prague, Czech Republic
[7]Czech Technical University in Prague, Prague, Czech Republic
[8]Institute of Physics, Academy of Sciences of the Czech Republic, Prague, Czech Republic
[9]Universidad San Francisco de Quito, Quito, Ecuador
[10]LPC, Université Blaise Pascal, CNRS/IN2P3, Clermont, France
[11]LPSC, Université Joseph Fourier Grenoble 1, CNRS/IN2P3, Institut National Polytechnique de Grenoble, Grenoble, France
[12]CPPM, Aix-Marseille Université, CNRS/IN2P3, Marseille, France
[13]LAL, Université Paris-Sud, CNRS/IN2P3, Orsay, France
[14]LPNHE, Universités Paris VI and VII, CNRS/IN2P3, Paris, France
[15]CEA, Irfu, SPP, Saclay, France
[16]IPHC, Université de Strasbourg, CNRS/IN2P3, Strasbourg, France
[17]IPNL, Université Lyon 1, CNRS/IN2P3, Villeurbanne, France and Université de Lyon, Lyon, France
[18]III. Physikalisches Institut A, RWTH Aachen University, Aachen, Germany
[19]Physikalisches Institut, Universität Freiburg, Freiburg, Germany
[20]II. Physikalisches Institut, Georg-August-Universität Göttingen, Göttingen, Germany
[21]Institut für Physik, Universität Mainz, Mainz, Germany
[22]Ludwig-Maximilians-Universität München, München, Germany
[23]Panjab University, Chandigarh, India
[24]Delhi University, Delhi, India
[25]Tata Institute of Fundamental Research, Mumbai, India
[26]University College Dublin, Dublin, Ireland
[27]Korea Detector Laboratory, Korea University, Seoul, Korea
[28]CINVESTAV, Mexico City, Mexico
[29]Nikhef, Science Park, Amsterdam, the Netherlands
[30]Radboud University Nijmegen, Nijmegen, the Netherlands
[31]Joint Institute for Nuclear Research, Dubna, Russia
[32]Institute for Theoretical and Experimental Physics, Moscow, Russia
[33]Moscow State University, Moscow, Russia
[34]Institute for High Energy Physics, Protvino, Russia
[35]Petersburg Nuclear Physics Institute, St. Petersburg, Russia
[36]Institució Catalana de Recerca i Estudis Avançats (ICREA) and Institut de Física d'Altes Energies (IFAE), Barcelona, Spain
[37]Uppsala University, Uppsala, Sweden
[38]Taras Shevchenko National University of Kyiv, Kiev, Ukraine
[39]Lancaster University, Lancaster LA1 4YB, United Kingdom
[40]Imperial College London, London SW7 2AZ, United Kingdom
[41]The University of Manchester, Manchester M13 9PL, United Kingdom
[42]University of Arizona, Tucson, Arizona 85721, USA
[43]University of California Riverside, Riverside, California 92521, USA
[44]Florida State University, Tallahassee, Florida 32306, USA
[45]Fermi National Accelerator Laboratory, Batavia, Illinois 60510, USA
[46]University of Illinois at Chicago, Chicago, Illinois 60607, USA
[47]Northern Illinois University, DeKalb, Illinois 60115, USA
[48]Northwestern University, Evanston, Illinois 60208, USA
[49]Indiana University, Bloomington, Indiana 47405, USA
[50]Purdue University Calumet, Hammond, Indiana 46323, USA
[51]University of Notre Dame, Notre Dame, Indiana 46556, USA
[52]Iowa State University, Ames, Iowa 50011, USA
[53]University of Kansas, Lawrence, Kansas 66045, USA
[54]Louisiana Tech University, Ruston, Louisiana 71272, USA
[55]Northeastern University, Boston, Massachusetts 02115, USA
[56]University of Michigan, Ann Arbor, Michigan 48109, USA
[57]Michigan State University, East Lansing, Michigan 48824, USA
[58]University of Mississippi, University, Mississippi 38677, USA
[59]University of Nebraska, Lincoln, Nebraska 68588, USA
[60]Rutgers University, Piscataway, New Jersey 08855, USA

[61]Princeton University, Princeton, New Jersey 08544, USA
[62]State University of New York, Buffalo, New York 14260, USA
[63]University of Rochester, Rochester, New York 14627, USA
[64]State University of New York, Stony Brook, New York 11794, USA
[65]Brookhaven National Laboratory, Upton, New York 11973, USA
[66]Langston University, Langston, Oklahoma 73050, USA
[67]University of Oklahoma, Norman, Oklahoma 73019, USA
[68]Oklahoma State University, Stillwater, Oklahoma 74078, USA
[69]Brown University, Providence, Rhode Island 02912, USA
[70]University of Texas, Arlington, Texas 76019, USA
[71]Southern Methodist University, Dallas, Texas 75275, USA
[72]Rice University, Houston, Texas 77005, USA
[73]University of Virginia, Charlottesville, Virginia 22904, USA
[74]University of Washington, Seattle, Washington 98195, USA

(Received 7 October 2014; revised manuscript received 1 December 2014; published 9 February 2015)

We present an updated measurement of the B_s^0 lifetime using the semileptonic decays $B_s^0 \to D_s^- \mu^+ \nu X$, with $D_s^- \to \phi\pi^-$ and $\phi \to K^+K^-$ (and the charge conjugate process). This measurement uses the full Tevatron Run II sample of proton-antiproton collisions at $\sqrt{s} = 1.96$ TeV, comprising an integrated luminosity of 10.4 fb^{-1}. We find a flavor-specific lifetime $\tau_{\rm fs}(B_s^0) = 1.479 \pm 0.010({\rm stat}) \pm 0.021({\rm syst})$ ps. This technique is also used to determine the B^0 lifetime using the analogous $B^0 \to D^- \mu^+ \nu X$ decay with $D^- \to \phi\pi^-$ and $\phi \to K^+K^-$, yielding $\tau(B^0) = 1.534 \pm 0.019({\rm stat}) \pm 0.021({\rm syst})$ ps. Both measurements are consistent with the current world averages, and the B_s^0 lifetime measurement is one of the most precise to date. Taking advantage of the cancellation of systematic uncertainties, we determine the lifetime ratio $\tau_{\rm fs}(B_s^0)/\tau(B^0) = 0.964 \pm 0.013({\rm stat}) \pm 0.007({\rm syst})$.

DOI: 10.1103/PhysRevLett.114.062001 PACS numbers: 14.40.Nd, 13.20.He

The decays of hadrons containing a b quark are dominated by the weak interaction of the b quark. In first-order calculations, the decay widths of these hadrons are independent of the flavor of the accompanying light quark(s). Higher-order predictions break this symmetry, with the spectator quarks having roles in the time evolution of the B hadron decay [1,2]. The flavor dependence leads to an expected lifetime hierarchy of $\tau(B_c) < \tau(\Lambda_b) < \tau(B_s^0) \approx \tau(B^0) < \tau(B^+)$, which has been observed experimentally [3]. The ratios of the lifetimes of different b hadrons are precisely predicted by heavy quark effective theories and provide a way to experimentally study these higher-order effects, and to test for possible new physics beyond the standard model [4]. Existing measurements are in excellent agreement with predictions [3] for the lifetime ratio $\tau(B^+)/\tau(B^0)$, but until recently the experimental precision has been insufficient to test the corresponding theoretical prediction for $\tau(B_s^0)/\tau(B^0)$. In particular, predictions using inputs from unquenched lattice QCD calculations give $0.996 < \tau(B_s^0)/\tau(B^0) < 1$ [2]. More precise measurements of both B_s^0 lifetime and the ratio to its lighter counterparts are needed to test and refine the models.

A flavor-specific final state such as $B_s^0 \to D_s^- \mu^+ \nu$ is one where the charges of the decay products can be used to know whether the meson was a B_s^0 or $\bar{B}_s^0$ at the time of decay. As a consequence of neutral B meson flavor oscillations, the B_s^0 lifetime as measured in semileptonic decays is actually a combination of the lifetimes of the heavy and light mass eigenstates with an equal mixture of these two states at time $t = 0$. If the resulting superposition of two exponential distributions is fitted with a single exponential function, one obtains to second order [5]

$$\tau_{\rm fs}(B_s^0) = \frac{1}{\Gamma_s} \frac{1 + (\Delta\Gamma_s/2\Gamma_s)^2}{1 - (\Delta\Gamma_s/2\Gamma_s)^2}, \quad (1)$$

where $\Gamma_s = (\Gamma_{sL} + \Gamma_{sH})/2$ is the average decay width of the light and heavy states, and $\Delta\Gamma_s$ is the difference $\Gamma_{sL} - \Gamma_{sH}$. This dependence makes the flavor-specific lifetime an important parameter in global fits [6] used to extract $\Delta\Gamma_s$, and hence, to constrain possible CP violation in the mixing and interference of B_s^0 mesons.

Previous measurements have been performed by the CDF [7], D0 [8], and LHCb [9,10] Collaborations, with additional earlier measurements from LEP [11]. During Run II of the Tevatron collider from 2002–2011, the D0 detector [12] accumulated 10.4 fb^{-1} of $p\bar{p}$ collisions at a center-of-mass energy of 1.96 TeV. We present a precise measurement of the B_s^0 lifetime that uses the flavor-specific decay $B_s^0 \to D_s^- \mu^+ \nu X$, with $D_s^- \to \phi\pi^-$ and $\phi \to K^+K^-$ [13], selected from this dataset. It is superseding our previous measurement [8].

A detailed description of the D0 detector can be found elsewhere [12]. The data for this analysis were collected with a single muon trigger. Events are considered for selection if they contain a muon candidate identified

through signatures both inside and outside the toroid magnet [12]. The muon must be associated with a central track, have transverse momentum (p_T) exceeding 2.0 GeV/c, and a total momentum of $p > 3.0$ GeV/c. Candidate $B_s^0 \to D_s^- \mu^+ \nu X$ decays are reconstructed by first combining two charged particle tracks of opposite charge, which are assigned the charged kaon mass. Both tracks must satisfy $p_T > 1.0$ GeV/c, and the invariant mass of the two-kaon system must be consistent with a ϕ meson, $1.008\ \text{GeV}/c^2 < M(K^+K^-) < 1.032\ \text{GeV}/c^2$. This ϕ candidate is then combined with a third track, assigned the charged pion mass, to form a $D_s^- \to \phi\pi^-$ candidate. The pion candidate must have $p_T > 0.7$ GeV/c, and the invariant mass of the $\phi\pi^-$ system must lie within a window that includes the D_s^- meson, $1.73\ \text{GeV}/c^2 < M(\phi\pi^-) < 2.18\ \text{GeV}/c^2$. The combinatorial background is reduced by requiring that the three tracks create a common D_s^- vertex as described in Ref. [14]. Lastly, each D_s^- meson candidate is combined with the muon to reconstruct a B_s^0 candidate. The invariant mass must be within the range $3\ \text{GeV}/c^2 < M(D_s^-\mu^+) < 5\ \text{GeV}/c^2$. All four tracks must be associated with the same $p\bar{p}$ interaction vertex (PV), and have hits in the silicon and fiber tracker detectors.

Muon and pion tracks from genuine B_s^0 decays must have opposite charges, which defines the right-sign sample. The wrong-sign sample is also retained to help constrain the background model. In the right-sign sample, the reconstructed D_s^- meson is required to be displaced from the PV in the same direction as its momentum in order to reduce background.

The flavor-specific B_s^0 lifetime, $\tau(B_s^0)$, can be related to the decay kinematics in the transverse plane, $c\tau(B_s^0) = L_{xy} M / p_T(B_s^0)$, where M is the B_s^0 mass, taken as the world average [3], and $L_{xy} = \vec{X} \cdot \vec{p}_T / |\vec{p}_T|$ is the transverse decay length, where $\vec{X}$ is the displacement vector from the PV to the secondary vertex in the transverse plane. Since the neutrino is not detected, and the soft hadrons and photons from decays of excited charmed states are not explicitly included in the reconstruction, the p_T of the B_s^0 meson cannot be fully reconstructed. Instead, we use the combined p_T of the muon and D_s^- meson, $p_T(D_s^-\mu^+)$. The reconstructed parameter is the pseudoproper decay length, $\text{PPDL} = L_{xy} M / p_T(D_s^-\mu^+)$. To model the effects of the missing p_T and of the momentum resolution when the B_s^0 lifetime is extracted from the PPDL distribution, a correction factor K is introduced, defined by $K = p_T(D_s^-\mu^+)/p_T(B_s^0)$. It is extracted from a Monte Carlo (MC) simulation, separately for a number of specific decays comprising both signal and background components.

MC samples are produced using the PYTHIA event generator [15] to model the production and hadronization phase, interfaced with EVTGEN [16] to model the decays of b and c hadrons. The events are passed through a detailed GEANT simulation of the detector [17] and additional algorithms to reproduce the effects of digitization, detector noise, and pileup. All selection cuts described above are applied to the simulated events. To ensure that the simulation fully describes the data, and in particular, to account for the effect of muon triggers, we weight the MC events to reproduce the muon transverse momentum distribution observed in data.

TABLE I. Relative contributions to the $D_s^-\mu^+$ signal from different semileptonic B_s^0 decays. The uncertainties are dominated by limited knowledge of the branching fractions [3,16]. In total, these processes comprise $(80.5 \pm 2.1)\%$ of the events in the $D_s^-\mu^+$ mass broad peak after subtracting combinatorial background.

Decay channel	Contribution
$D_s^-\mu^+\nu_\mu$	$(27.5 \pm 2.4)\%$
$D_s^{*-}\mu^+\nu_\mu \times (D_s^{*-} \to D_s^-\gamma / D_s^-\pi^0)$	$(66.2 \pm 4.4)\%$
$D_{s(J)}^{*-}\mu^+\nu_\mu \times (D_{s(J)}^{*-} \to D_s^{*-}\pi^0 / D_s^{*-}\gamma)$	$(0.4 \pm 5.3)\%$
$D_s^{(*)-}\tau^+\nu_\tau \times (\tau^+ \to \mu^+\bar{\nu}_\mu\nu_\tau)$	$(5.9 \pm 2.7)\%$

Table I summarizes the semileptonic B_s^0 decays that contribute to the $D_s^-\mu^+$ signal. Experimentally, these processes differ only in the varying amount of energy lost to missing decay products, which is reflected in the final K-factor distribution. Table II shows the list of non-negligible processes from subsequent semileptonic charm decays which also contribute to the signal. These two tables represent the sample composition of the $D_s^-\mu^+$ signal.

We partition the dataset into five data-collection periods, separated by accelerator shutdowns, each comprising 1–3 fb^{-1} of integrated luminosity, to take into account time- or luminosity-dependent effects. The behavior and overall contribution of the dominant combinatorial backgrounds changed as the collider, detector, and trigger conditions evolved over the course of the Tevatron Run II. Figure 1 shows the $M(\phi\pi^-)$ invariant mass distribution for the right-sign $D_s^-\mu^+$ candidates for one of these data periods. Lifetimes are extracted separately for each period; they are consistent within uncertainties and a weighted average is made for the final measurement. The MC weighting as a function of p_T is performed separately

TABLE II. Other semileptonic decays contributing to the $D_s^-\mu^+$ signal. Listed contributions are obtained after subtracting combinatorial background. The uncertainties are dominated by limited knowledge of the branching fractions [3,16].

Decay channel	Contribution
$B^+ \to D_s^- DX$	$(3.81 \pm 0.75)\%$
$B^0 \to D_s^- DX$	$(4.13 \pm 0.70)\%$
$B_s^0 \to D_s^- D_s^{(*)} X$	$(1.11 \pm 0.36)\%$
$B_s^0 \to D_s^- DX$	$(0.92 \pm 0.44)\%$
$c\bar{c} \to D_s^-\mu^+$	$(9.53 \pm 1.65)\%$

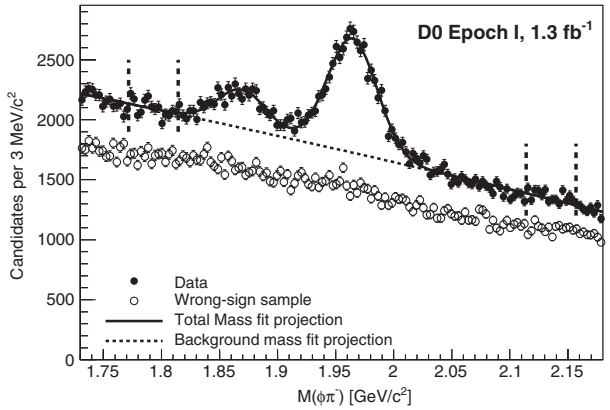

FIG. 1. Distributions of the invariant mass $M(\phi\pi^-)$ for $D_s^-\mu^+$ candidates passing all selection criteria in one of the five data periods. The higher-mass peak is the D_s^- signal, with a smaller D^- peak at lower mass. Sidebands for right-sign sample are indicated with dashed lines and the corresponding distribution for the wrong-sign sample is also shown.

for each of the five data samples. The K factors are extracted independently in each sample, with significant shifts observed due to the changing trigger conditions. The K-factor distribution peaks at ≈ 0.9 for the D_s^- signal and at ≈ 0.8 for the first four backgrounds listed in Table II. The K-factor distribution populates $0.5 < K < 1$ for both the signal and background components.

To determine the number of events in the signal region and define the signal and background samples, we fit a model to the $M(\phi\pi^-)$ invariant mass distribution as shown in Fig. 1. The D_s^- and D^- mass peaks are each modeled using an independent Gaussian distribution to represent the detector mass resolution, and a second-order polynomial is used to model the combinatorial background. Using the information obtained from these fits, we define the signal sample (SS) as those events in the $M(\phi\pi^-)$ mass distribution that are within $\pm 2\sigma$ of the fitted mean D_s^- meson mass, where σ is the Gaussian width of the D_s^- mass peak obtained from the fit. We find a total of 72028 ± 727 $D_s^-\mu^+$ signal events in the full dataset. Yields observed in the different periods are consistent with expectations taking into account changing trigger conditions and detector performance. The background sample (BS) includes those events in the sidebands of the D_s^- mass distribution given by -9σ to -7σ and $+7\sigma$ to $+9\sigma$ from the fitted mean mass. Wrong-sign events in the full $M(\phi\pi^-)$ range are also included in the background sample, yielding more events to constrain the behavior of the combinatorial background.

The extraction of the flavor-specific B_s^0 lifetime is performed using an unbinned maximum likelihood fit to the data, based on the PPDL of each candidate [18]. The effects of finite L_{xy} resolution of the detector and the K factors are included in this fit to relate the underlying decay time of the candidates to the corresponding observed quantity. The signal and background samples defined above are fitted simultaneously, with a single shared set of parameters used to model the combinatorial background shape. To validate the lifetime measurement method, we perform a simultaneous fit of the B^0 lifetime using the Cabibbo suppressed decay $B^0 \to D^-\mu^+X$ seen in Fig. 1 at lower masses. This measurement also enables the ratio $\tau_{\rm fs}(B_s^0)/\tau(B^0)$ to be measured with high precision, since the dominant systematic uncertainties are highly correlated between the two lifetime measurements. For simplicity, the details of the fitting function are illustrated for the B_s^0 lifetime fit alone. In practice, an additional likelihood product is included to extract the B^0 lifetime in an identical manner.

The likelihood function $\mathcal{L}$ is defined as

$$\mathcal{L} = \prod_{i\in \rm SS} [f_{D_s\mu}\mathcal{F}^i_{D_s\mu} + (1 - f_{D_s\mu})\mathcal{F}^i_{\rm comb}] \prod_{j\in \rm BS} \mathcal{F}^j_{\rm comb}, \quad (2)$$

where $f_{D_s\mu}$ is the fraction of $D_s^-\mu^+$ candidate events in the signal sample, obtained from the fit of the D_s^- mass distribution, and $\mathcal{F}^i_{D_s\mu({\rm comb})}$ is the candidate (combinatorial background) probability density function (PDF) evaluated for the ith event. The probability density $\mathcal{F}^i_{D_s\mu}$ is given by

$$\mathcal{F}^i_{D_s\mu} = f_{\bar{c}c}F^i_{\bar{c}c} + f_{B1}F^i_{B1} + f_{B2}F^i_{B2} + f_{B3}F^i_{B3} + f_{B4}F^i_{B4} + (1 - f_{\bar{c}c} - f_{B1} - f_{B2} - f_{B3} - f_{B4})F^i_s. \quad (3)$$

Each factor f_X is the expected fraction of a particular component X in the signal sample, obtained from simulations and listed in Tables I and II. The first term accounts for the prompt $c\bar{c}$ component, and the decays $B1$–$B2$ represent the first four components listed in Table II. The last term of the sum in Eq. (3) represents the signal events $S \equiv (B_s^0 \to D_s^-\mu^+\nu X)$ listed in Table I. The factor $F_{\bar{c}c}$ is the lifetime PDF for the $\bar{c}c$ events, given by a Gaussian distribution with a mean of zero and a free width. Each B decay mode is associated with a separate PDF, F_X, modeling the PPDL distribution, given by an exponential decay convoluted with a resolution function and with the K-factor distribution. All B-meson decays are subject to the same PPDL resolution function. A double-Gaussian distribution is used for the resolution function, with widths given by the event-by-event PPDL uncertainty determined from the B_s^0 candidate vertex fit multiplied by two overall scale factors and a ratio between their contributions that are all allowed to vary in the fit.

The combinatorial background PDF, $\mathcal{F}_{\rm comb}$, is chosen empirically to provide a good fit to the combinatorial background PPDL distribution. It is defined as the sum of the double-Gaussian resolution function and two exponential decay functions for both the positive and negative PPDL regions. The shorter-lived exponential decays are fixed to have the same slope for positive and negative regions, while different slopes are allowed for the longer-lived exponential decays. Figure 2 shows the PPDL

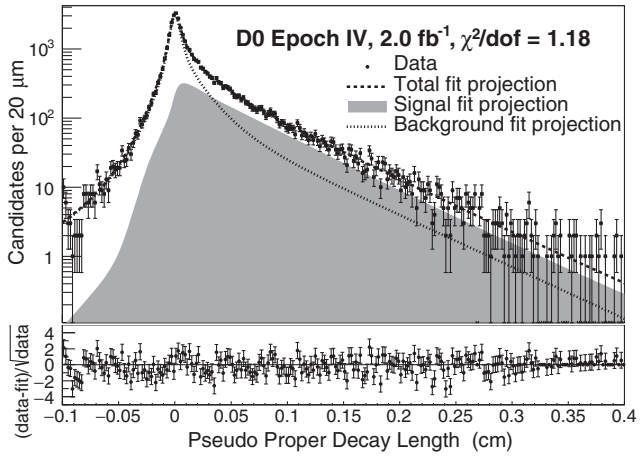

FIG. 2. Top: PPDL distribution for $D_s^- \mu^+$ candidates in the signal sample for one of the five data periods. The projections of the lifetime fitting model, the background function, and the signal function are superimposed. Bottom: fit residuals demonstrating the agreement between the data and the fit model

distribution for one of the five data periods for the signal sample, along with the comparison with the fit model. The corresponding χ^2 per degree of freedom for each data-taking period are 1.58,1.21,1.29,1.18, and 1.14.

The corresponding B^0 lifetime measurement uses exactly the same procedure for events in the D^- mass peak, including a calculation of dedicated K factors and background contributions from semileptonic decays.

The lifetime fitting procedure is tested using MC pseudoexperiments, in which the generated $B^0_{(s)}$ lifetime is set to a range of different values, and the full fit is performed on the simulated data. Good agreement is found between the input and extracted lifetimes in all cases. As an additional cross-check, the data are divided into pairs of subsamples, and the fit is performed separately for both samples. The divisions correspond to low and high $p_T(B^0_{(s)})$, central and forward pseudorapidity $|\eta(B^0_{(s)})|$ regions, and $B^0_{(s)}$ versus $\bar{B}^0_{(s)}$ decays. In all cases, the measured lifetimes are consistent within uncertainties.

To evaluate systematic uncertainties on the measurements of $c\tau(B^0_s)$, $c\tau(B^0)$, and the ratio $\tau_{\rm fs}(B^0_s)/\tau(B^0)$, we consider the following possible sources: modeling of the decay length resolution, combinatorial background evaluation, K-factor determination, background contribution from charm semileptonic decays, signal fraction, and alignment of the detector. All other sources investigated are found to be negligible. The effect of possible mismodeling of the decay length resolution is tested by repeating the lifetime fit with alternative resolution models, using a single Gaussian component. A systematic uncertainty is assigned based on the shift in the measured lifetime. We repeat the fit using different combinatorial background samples using only the sideband data or only the wrong-sign sample. The maximum deviation from the central lifetime measurement is assigned as a systematic uncertainty. To determine the effect of uncertainties on the K factors for the signal events, the fractions of the different components are varied within their uncertainties given in Table I. We also recalculate the K factors using different MC decay models [16], leading to a harder p_T distribution of the generated B hadrons. The fraction of each component from semileptonic decays is varied within its uncertainties, and the shift in the measured lifetime is used to assign a systematic uncertainty. The signal fraction parameter, $f_{D_s\mu}$, is fixed for each mass fit performed. We vary this parameter within its statistical and systematic uncertainty, obtained from fit variations to the background and signal model of the mass PDFs, and assign the observed deviation as the uncertainty arising from this source. Finally, to assess the effect of possible detector misalignment, a single MC sample is passed through two different reconstruction algorithms, corresponding to the nominal detector alignment and an alternative model with tracking detector elements shifted spatially within their uncertainties. The observed change in the lifetime is taken as systematic uncertainty due to alignment.

Table III lists the contributions to the systematic uncertainty from all sources considered. The most significant effect comes from the combinatorial background determination. Correlations in the systematic uncertainties for the B^0_s and B^0 meson lifetimes are taken into account when evaluating the effect on the lifetime ratio, where the K factor determination dominates.

The measured flavor-specific lifetime of the B^0_s meson is $c\tau_{\rm fs}(B^0_s) = 443.3 \pm 2.9({\rm stat}) \pm 6.3({\rm syst})\ \mu{\rm m}$, which is consistent with the current world average of $439.2 \pm 9.3\ \mu$m [3,6] and has a smaller total uncertainty of $6.9\ \mu$m. The uncertainty in this measurement is dominated by systematic effects. The B^0 lifetime in the semileptonic decay $B^0 \to D^- \mu^+ \nu X$ is measured to be $c\tau(B^0) = 459.8 \pm 5.6({\rm stat}) \pm 6.4({\rm syst})\ \mu{\rm m}$, consistent with the world average of $c\tau(B^0) = 455.4 \pm 1.5\ \mu$m [3]. Using both lifetimes obtained in the current analysis, their ratio is determined to be $\tau_{\rm fs}(B^0_s)/\tau(B^0) = 0.964 \pm 0.013({\rm stat}) \pm 0.007({\rm syst})$. Both results are in reasonable agreement with theoretical predictions from lattice QCD [1,2]; the flavor-specific

TABLE III. Summary of systematic uncertainty contributions to the B^0_s and B^0 lifetimes, and to the ratio $R \equiv \tau_{\rm fs}(B^0_s)/\tau(B^0)$.

Uncertainty source	$\Delta(c\tau_{B^0_s})\mu$m	$\Delta(c\tau_{B^0})\mu$m	ΔR
Resolution	0.7	2.1	0.003
Combinatorial background	5.0	4.9	0.001
K factor	1.6	1.3	0.006
Semileptonic components	2.6	2.0	0.001
Signal fraction	1.0	1.8	0.002
Alignment of the detector	2.0	2.0	0.000
Total	6.3	6.4	0.007

lifetime has a better precision than the current world average [3,6], and agrees reasonably well with the slightly more precise recent measurement from the LHCb Collaboration [10].

In summary, we measure the B_s^0 lifetime in the inclusive semileptonic channel $B_s^0 \to D_s^- \mu^+ \nu X$ and obtain one of the most precise determinations of the flavor-specific B_s^0 lifetime. Combining this result and that of Ref. [10] with global fits of lifetime measurements in $B_s^0 \to J/\psi K^+ K^-$ decays [6] gives the most precise determination of the fundamental parameters $\Delta\Gamma_s$ and Γ_s which are important for constraining CP violation in the B_s^0 system. Our precise measurement of the ratio of B_s^0 and B^0 lifetimes can be used to test and refine theoretical QCD predictions and offers a sensitive test of new physics [4].

We thank the staffs at Fermilab and collaborating institutions, and acknowledge support from the Department of Energy and National Science Foundation (United States of America); Alternative Energies and Atomic Energy Commission and National Center for Scientific Research/National Institute of Nuclear and Particle Physics (France); Ministry of Education and Science of the Russian Federation, National Research Center "Kurchatov Institute" of the Russian Federation, and Russian Foundation for Basic Research (Russia); National Council for the Development of Science and Technology and Carlos Chagas Filho Foundation for the Support of Research in the State of Rio de Janeiro (Brazil); Department of Atomic Energy and Department of Science and Technology (India); Administrative Department of Science, Technology, and Innovation (Colombia); National Council of Science and Technology (Mexico); National Research Foundation of Korea (Korea); Foundation for Fundamental Research on Matter (The Netherlands); Science and Technology Facilities Council and The Royal Society (United Kingdom); Ministry of Education, Youth and Sports (Czech Republic); Bundesministerium für Bildung und Forschung (Federal Ministry of Education and Research) and Deutsche Forschungsgemeinschaft (German Research Foundation) (Germany); Science Foundation Ireland (Ireland); Swedish Research Council (Sweden); China Academy of Sciences and National Natural Science Foundation of China (China); and Ministry of Education and Science of Ukraine (Ukraine).

[a]Visitor from Augustana College, Sioux Falls, SD, USA.
[b]Visitor from The University of Liverpool, Liverpool, UK.
[c]Visitor from DESY, Hamburg, Germany.
[d]Visitor from Universidad Michoacana de San Nicolas de Hidalgo, Morelia, Mexico.
[e]Visitor from SLAC, Menlo Park, CA, USA.
[f]Visitor from University College London, London, UK.
[g]Visitor from Centro de Investigacion en Computacion-IPN, Mexico City, Mexico.
[h]Visitor from Universidade Estadual Paulista, São Paulo, Brazil.
[i]Visitor from Karlsruher Institut für Technologie (KIT)-Steinbuch Centre for Computing (SCC), D-76128 Karlsruhe, Germany.
[j]Visitor from Office of Science, U.S. Department of Energy, Washington, D.C. 20585, USA.
[k]Visitor from American Association for the Advancement of Science, Washington, D.C. 20005, USA.
[l]Visitor from Kiev Institute for Nuclear Research, Kiev, Ukraine.
[m]Visitor from University of Maryland, College Park, Maryland 20742, USA.
[n]Visitor from European Organization for Nuclear Research (CERN), Geneva, Switzerland.

[1] D. Becirevic, *Proc. Sci.*, HEP (2001) 098; M. Neubert and C. T. Sachrajda, Nucl. Phys. **B483**, 339 (1997).
[2] A. Lenz and U. Nierste, J. High Energy Phys. 06 (2007) 072 (and recent update arXiv:1102.4274).
[3] K. A. Olive *et al.* (Particle Data Group), Chin. Phys. C **38**, 090001 (2014).
[4] C. Bobeth, U. Haisch, A. Lenz, B. Pecjak, and G. Tetlalmatzi-Xolocotzi, J. High Energy Phys. 06 (2014) 040.
[5] K. Hartkorn and H.-G. Moser, Eur. Phys. J. C **8**, 381 (1999).
[6] Y. Amhis *et al.* (Heavy Flavor Averaging Group Collaboration), arXiv:1207.1158, with web update at http://www.slac.stanford.edu/xorg/hfag/osc/PDG_2014/.
[7] T. Aaltonen *et al.* (CDF Collaboration), Phys. Rev. Lett. **107**, 272001 (2011); F. Abe *et al.* (CDF Collaboration), Phys. Rev. D **59**, 032004 (1999).
[8] V. M. Abazov *et al.* (D0 Collaboration), Phys. Rev. Lett. **97**, 241801 (2006).
[9] R. Aaij *et al.* (LHCb Collaboration), Phys. Rev. Lett. **112**, 111802 (2014); R. Aaij *et al.* (LHCb Collaboration), Phys. Lett. B **736**, 446 (2014).
[10] R. Aaij *et al.* (LHCb Collaboration), Phys. Rev. Lett. **113**, 172001 (2014).
[11] P. Abreu *et al.* (DELPHI Collaboration), Eur. Phys. J. C **16**, 555 (2000); K. Ackerstaff *et al.* (OPAL Collaboration), Phys. Lett. B **426**, 161 (1998); D. Buskulic *et al.* (ALEPH Collaboration), Phys. Lett. B **377**, 205 (1996).
[12] V. M. Abazov *et al.* (D0 Collaboration), Nucl. Instrum. Methods Phys. Res., Sect. A **565**, 463 (2006).
[13] Charge conjugation is implied throughout this article.
[14] J. Abdallah *et al.* (DELPHI Collaboration), Eur. Phys. J. C **32**, 185 (2004).
[15] T. Sjöstrand, P. Edén, C. Friberg, L. Lönnblad, G. Miu, S. Mrenna, and E. Norrbin, Comput. Phys. Commun. **135**, 238 (2001). We use version 6.409.
[16] D. J. Lange, Nucl. Instrum. Methods Phys. Res., Sect. A **462**, 152 (2001).
[17] R. Brun *et al.*, CERN Report No. CERN-DD-EE-84-1 1987.
[18] J. Martínez Ortega, Ph.D. thesis, Cinvestav, [FERMILAB-THESIS-2012-60, 2012 (unpublished)] http://inspirehep.net/record/1315759.